AMERICAN JOURNAL OF PHYSICAL ANTHROPOLOGY 149:365–379 (2012)

The Mousterian Child From Teshik-Tash is a Neanderthal: A Geometric Morphometric Study of the Frontal Bone

Philipp Gunz[1] and Ekaterina Bulygina[2]

[1]*Department of Human Evolution, Max Planck Institute for Evolutionary Anthropology, Deutscher Platz 6, D-04103 Leipzig, Germany*
[2]*Anuchin's Anthropology Museum MSU, Moscow, 125009 Russia*

KEY WORDS procrustes; semilandmarks; developmental simulation; hominin; evolution

ABSTRACT In the 1930s subadult hominin remains and Mousterian artifacts were discovered in the Teshik-Tash cave in South Uzbekistan. Since then, the majority of the scientific community has interpreted Teshik-Tash as a Neanderthal. However, some have considered aspects of the morphology of the Teshik-Tash skull to be more similar to fossil modern humans such as those represented at Skhūl and Qafzeh, or to subadult Upper Paleolithic modern humans. Here we present a 3D geometric morphometric analysis of the Teshik-Tash frontal bone in the context of developmental shape changes in recent modern humans, Neanderthals, and early modern humans. We assess the phenetic affinities of Teshik-Tash to other subadult fossils, and use developmental simulations to predict possible adult shapes. We find that the morphology of the frontal bone places the Teshik-Tash child close to other Neanderthal children and that the simulated adult shapes are closest to Neanderthal adults. Taken together with genetic data showing that Teshik-Tash carried mtDNA of the Neanderthal type, as well as its occipital bun, and its shovel-shaped upper incisors, these independent lines of evidence firmly place Teshik-Tash among Neanderthals. Am J Phys Anthropol 149:365–379, 2012.

Hominin remains were recovered during the excavations of 1938 by A.P. Okladnikov in the Teshik-Tash cave, in the Gissar Mountain Range of South Uzbekistan. The cave contained up to five cultural layers bearing Mousterian artifacts. The hominin fossils were found underneath the first upper cultural level (Okladnikov, 1949). The excavators claimed that the human remains were found near a hearth contained in this cultural level. The skull was squashed by the overlying matter into hundreds of fragments that were found in close proximity. The Teshik-Tash hominin comprises a virtually complete cranium (Fig. 1), which was reconstructed from about 150 pieces by M.M. Gerasimov, an almost complete mandible, and a number of postcranial elements. The postcranial remains include fragments of vertebrae (including a complete atlas), clavicles (the left one is complete), fragments of ribs, fragments of an ischium, the diaphyses of both femora, fragments of the tibial diaphysis, the diaphysis of the left humerus and a number of unidentifiable fragments (Gremiatsky, 1949; Sinel'nikov and Gremiatsky, 1949). It has been suggested that the loss of the majority of the child's body parts was due to carnivore activity when the cave was abandoned.

The preliminary suggestion of a Middle Palaeolithic age of the site was based on the Mousterian type of cultural artifacts and the archaic morphology of the human remains. The faunal remains were found to be similar to modern specimens and were therefore not useful for dating purposes. It was therefore hypothesized that the occupation of the cave must have occurred during one of the latest interglacial periods (most possibly Mindel-Riss), when the climate of Central Asia was similar to the present day. Recent attempts at radiocarbon dating of the Teshik-Tash remains have not changed their initial assignment to the Middle Palaeolithic age (T. Higham, personal communication). During the 2-year excavations in 1938–1939 the whole cave was cleaned out and all cultural levels were removed, rendering any new study of the cave impossible.

According to a detailed comparative analysis of the skull by Gremiatsky (1949), the dental age of the child is equivalent to 8–9 years of age of modern European children. However, Teshik-Tash was found to have a neurocranium that is relatively larger than in modern children of the same age; it also has a taller face. Gremiatsky therefore suggested that Neanderthals had a faster rate of growth than modern human children. Although the Teshik-Tash cranium was found to be relatively taller and its frontal bone to be more curved than in adult Neanderthals, Gremiatsky still considered its forehead to be flatter than in modern children and pointed out a number of archaic (or "pithecoid") features

Additional Supporting Information may be found in the online version of this article.

Philipp Gunz and Ekaterina Bulygina contributed equally to this work.

*Correspondence to: Philipp Gunz, Department of Human Evolution, Max Planck Institute for Evolutionary Anthropology, Deutscher Platz 6, D-04103 Leipzig, Germany or Ekaterina Bulygina. Anuchin's Anthropology Museum MSU, Moscow, Russia.
E-mail: gunz@eva.mpg.de or ebulygin@yahoo.com

Received 3 May 2012; accepted 23 July 2012

DOI 10.1002/ajpa.22133
Published online 14 September 2012 in Wiley Online Library (wileyonlinelibrary.com).

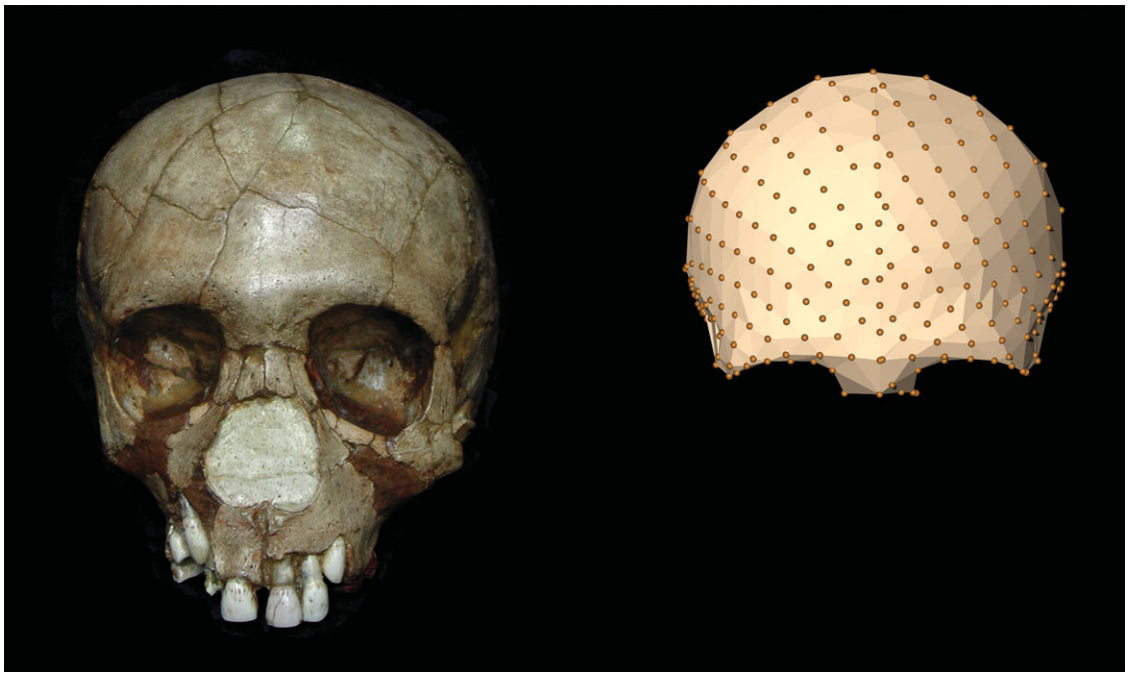

Fig. 1. Left: Teshik-Tash (picture of the original specimen). Right: Landmarks and semilandmarks on the frontal bone. [Color figure can be viewed in the online issue, which is available at wileyonlinelibrary.com.]

in the Teshik-Tash cranium and mandible: lack of the mental eminence, very high face, large teeth, absence of a canine fossae, the initial development of a prominent browridge, a small mastoid processes, and a low, posteriorly prominent occipital. In general, Gremiatsky (1949) found that the skull was similar to La Quina 18, a Neanderthal child ~1.5–2 years younger than the presumed age of Teshik-Tash (Smith et al., 2010). Most authors agree that Teshik-Tash remains belong to a subadult individual. Further studies of Teshik-Tash (Gremiatsky, 1949; Jelinek et al., 1969; Vlcek, 1991; Kharitonov, 2009) agreed that it displays some derived Neanderthal features (Stefan and Trinkaus, 1998; Rosas, 2001; Trinkaus, 2003; Trinkaus et al., 2006; Hublin, 2009), such as an occipital bun, an oval-shaped foramen magnum, taurodontism, and shovel-shaped upper incisors. The skull also exhibits several plesiomorphic Neanderthal features such as a supraorbital ridge and the absence of a chin. Several Neanderthal characteristics, however, such as the "en-bombe" shape of the neurocranium, are expressed to a lesser extent than in other Neanderthals. Other features, such as the position of the mental foramina and lingula of the mandibular foramen, were found to be more characteristic of modern humans than Neanderthals. This mosaic of morphological features has prompted some authors to question the Neanderthal affinities of Teshik-Tash: Weidenreich (1945) argued that Teshik-Tash has a closer morphological association with the Mount Carmel hominins from Skhūl and Qafzeh. It is worth remembering, however, that Weidenreich (1943, 1945) saw Neanderthals as being ancestral to modern humans, and considered the fossils from Skhūl and Qafzeh to be "intermediate" between Neanderthals and modern man. Wolpoff et al. (2004) regarded Teshik-Tash as an example of an eastern Neanderthal that lacks many of the European midfacial features distinguishing western Neanderthals from modern humans. Glantz et al. (2009) have shown that a multivariate statistical analysis of traditional morphometrics based on 27 linear measurements places the Teshik-Tash cranium and mandible outside the variation of subadult Neanderthals and associates it with subadult Upper Paleolithic humans. These authors argued that metric aspects of Teshik-Tash's unreconstructed morphology depart from the pattern observed in subadult European Neanderthals in both size and shape; however, Glantz et al. (2009) did not consider this evidence to be strong enough to warrant a reclassification of Teshik-Tash as an early human. If Teshik-Tash is not a typical Neanderthal (Wolpoff et al., 2004; Glantz et al., 2009), or no Neanderthal at all (Weidenreich, 1945), this obviously has implications for hominin population structure and dynamics in Central Asia (see also Dalén et al., 2012 for a genetic perspective). Specifically Glantz et al. (2009: p 58) argued that "the characterization of Central Asia as the eastern periphery of the Neanderthal range is likely an oversimplification of the actual pattern of regional variation across Eurasia during the Late Pleistocene." Moreover, this observation is important as the Teshik-Tash skull is frequently used in comparative studies to infer Neanderthal development (e.g., Minugh-Purvis, 1988; Stringer and Gamble, 1993; Ruff et al., 1994; Rak et al., 1994; Tillier, 1995, 1996; Ponce de León and Zollikofer, 2001; Williams, 2001; Williams et al., 2002a,b; Krovitz, 2003; Williams and Krovitz, 2004; Ponce de León et al., 2008; Kharitonov, 2009; Zollikofer and Ponce de León, 2010).

The Neanderthal affinity of the Teshik-Tash subadult has been recently confirmed by mtDNA analysis (Krause et al., 2007). The results of Glantz et al. (2009) are therefore particularly interesting in light of the recent interpretation of genetic evidence, which suggests admixture between Neanderthals and the ancestors of recent modern humans (Green et al., 2010). In a metric study of the shape of the scapular glenoid fossa Di Vincenzo et al.

(2012) showed that Near Eastern Neanderthals are similar to the modern condition and are somewhat segregated from both northwestern European and early Mediterranean Neanderthals. These authors suggested that these data are consistent with low levels of gene flow between Neanderthals and modern humans in the Near East.

The recent work on hominin remains from Obi-Rakhmat, Anghilak caves, and Okladnikov highlights the difficulty of classifying the currently known Central Asian findings due to the fragmentary nature of the remains and the absence of diagnostic Neanderthal features in the available material (Glantz et al., 2004, 2008; Viola et al., 2004; Bailey et al., 2008). Moreover, the discovery of "the Denisovans," a new fossil group for which only limited morphological information is currently known (Krause et al., 2010; Reich et al., 2010), adds yet another layer of complexity to the interpretation of the fossil record in Central Asia and hominin population dynamics (Otte, 2007; Glantz, 2010).

AIMS OF THIS STUDY

Here we reassess the phenetic affinities of Teshik-Tash to recent modern humans, West Asian fossil modern humans, and Neanderthals in a comparative context of developmental shape changes. We use 3D landmarks and hundreds of sliding semilandmarks to quantify the morphology of the frontal bone using geometric morphometrics. Here, we focus on the frontal bone morphology for two reasons:

1. As discussed in Glantz et al. (2009), the Teshik-Tash skull has been reconstructed from a large number of small pieces (Fig. 1). Its frontal bone is one of the few regions that preserve a tight articulation between fragments, and displays only limited taphonomic deformation.
2. Focusing on the frontal bone morphology made it possible to increase the size of the comparative fossil sample, in particular of Upper Paleolithic hominins.

We therefore study the frontal bone morphology of the Teshik-Tash subadult using 3D geometric morphometrics (Bookstein, 1991; Slice, 2007; Mitteroecker and Gunz, 2009). Several previous metric studies of frontal bone morphology found good discrimination among groups of modern humans and Pleistocene hominins (Cunningham, 1908; Smith and Ranyard, 1980; Lahr and Wright, 1996; Bulygina, 2007; Stansfield nee Bulygina and Gunz, 2011), whereas others highlighted its limitations in discriminating among Middle Pleistocene hominins (Athreya, 2006, 2009; Freidline et al., 2012).

Given the scarcity of comparable subadult fossil modern humans, we use developmental simulations (McNulty et al., 2006; Singleton et al., 2010) to predict possible adult shapes for Teshik-Tash. Predicting developmental trajectories on the basis of a sample of frontal bones, however, presents its challenges. The frontal bone encompasses two functionally different regions of the skull, the neurocranium and the upper face, which grow at different rates and different times. In modern humans, more than 90% of the adult neurocranial size is achieved by the M1 occlusion; facial growth and maturation, however, continue beyond this age 1 (Humphrey, 1998; Viðarsdóttir et al., 2002; Ackermann and Krovitz, 2002; Cobb and O'Higgins, 2004; Coqueugniot et al., 2004; Guihard-Costa and Ramírez Rozzi, 2004; Mitteroecker et al., 2004a,b; Viðarsdóttir and Cobb, 2004; Bulygina et al., 2006; Hublin and Coqueugniot, 2006; Cobb and O'Higgins, 2007; Coqueugniot and Hublin, 2007; DeSilva and Lesnik, 2008; Mitteroecker and Bookstein, 2009; Neubauer et al., 2009, 2010; Harvati et al., 2010; Gunz et al., 2010, 2011, 2012; Coqueugniot and Hublin, 2012; Leigh, 2012; Neubauer and Hublin, 2012; Neubauer et al., 2012a). Developmental trajectories of the frontal bone are therefore the result of a combination of two developmental processes (Mitteroecker et al., 2005; Mitteroecker and Bookstein, 2007, 2008), where size increase predates shape maturation.

Neanderthals differ from recent and terminal Pleistocene human populations in their patterns of dental development (Bayle et al., 2009, 2010). Dental evidence suggests that aspects of Neanderthal development were faster than in modern humans (Ramírez Rozzi and Bermudez De Castro, 2004; Ramírez Rozzi and Sardi, 2007; Smith et al., 2007a,b, 2010), although overlap exists (Guatelli-Steinberg et al., 2005; Macchiarelli et al., 2006). Bayle et al. (2009) reported a delayed mineralization of the incisors of the Neanderthal subadult from Roc de Marsal compared to modern humans, whereas the mineralization of the first molar was advanced. In our developmental simulations we therefore use broad stages of dental development as an independent variable rather than frontal bone size, or estimates of individual calendar age. We then assess the phenetic affinities of these simulated adults to adult Neanderthals and modern human fossils.

MATERIALS

Our sample comprises 123 recent modern human individuals from nine populations (93 adults and 30 subadults; see Supporting Information Table 1 and Stansfield and Gunz, 2011 for details on the sample); 6 early modern humans from the Levant (4 adults, 2 subadults); 14 Neanderthals (10 adults, 4 subadults); 20 Upper Palaeolithic modern humans; and 4 ungrouped fossils, including Teshik-Tash (Table 1). The recent modern human sample was selected to reflect the worldwide modern human shape variation. Each population contains both males and females; most populations include children of various ages. Most recent modern humans in the comparative sample come from archeological populations; sex and age determination was carried out by one of the authors (EB), following protocols in Buikstra and Ubelaker (1994) on the basis of dental development charts and dimorphic cranial features for each population separately.

METHODS

A detailed description of the entire measurement and data processing protocol for the frontal bone can be found in Stansfield nee Bulygina and Gunz (2011), therefore we only summarize the measurement protocol below. Nineteen anatomical landmarks (*midline landmarks*: bregma; glabella; nasion; *bilateral landmarks*: stephanion; sphenion; frontotemporale; frontomalare temporale; frontomalare anterior; frontomalare orbitale; maxillofrontale, dacryon), four curves and the whole frontal bone surface were collected by EB as three-dimensional coordinates with the help of a Microscribe 3DX digitizer. Semilandmarks were generated as initially equidistant points along curves; the surface-semilandmarks of the frontal (Fig. 2) were distributed following the protocol developed by Gunz (Gunz et al., 2005,

TABLE 1. Fossils sample

Name	Origin	Collection	Dental age	Dental stage	Reconstruction		
					Areas	Landmarks	Total landmarks and outline semilandmarks
Upper Paleolithic modern humans							
Abri Pataud	France	Musee de l'Homme, Paris	Adult	6	None	None	None
Cromagnon 1	France	Musee de l'Homme, Paris	Adult	6	Small area on the inside of the left medial orbital plate	Dacrion left	1
Cromagnon 2	France	Musee de l'Homme, Paris	Adult	6	None	None	None
Cromagnon 3	France	Musee de l'Homme, Paris	Adult	6	Small area on the inside of the right medial orbital plate	Dacrion right	3
Dolní Věstonice 1[a]	Czech Republic	Dolni Vestoniče Museum	Adult	6	Small distal part of the left temporal area, left zygomatic process, small lateral portion of the right, medial potions of the left and right orbits	Frontotemporale left, dacrion left and right, frontomalare anterior left and right, frontomalare orbitale left and right, frontomalare temporale left and right	12
Dolní Věstonice 3[a]	Czech Republic	Dolni Vestoniče Museum	Adult	6	None	None	None
Dolní Věstonice 15	Czech Republic	Dolni Vestoniče Museum	Adult	6	Small area on the inside of the right medial orbital plate	Dacrion right	5
Dolní Věstonice 16	Czech Republic	Dolni Vestoniče Museum	Adult	6	None	None	None
Mladeč 1	Czech Republic	Natural History Museum, Vienna	Adult	6	Left temporal area including about 2/3 of the left temporal line (both zygomatic processes, however, are mostly intact)	Stephanion right, frontotemporale right, sphenion right, dacrion right	14
Mladeč 2	Czech Republic	Natural History Museum, Vienna	Adult	6	Both distal temporal areas; distal portions of both zygomatic processes, including distal ends of the lateral orbital portions	Sphenion left and right, dacrion left and right, frontomalare anterior left and right, frontomalare orbitale left and right, frontomalare temporale left and right	26
Mladeč 5[a]	Czech Republic	Natural History Museum, London	Adult	6	Small areas on the inside of both medial orbital plates; distal ends of the lateral portions of the orbital rims on both sides	Dacrion left and right, frontomalare orbitale left and right	10
Pavlov	Czech Republic	Dolni Vestoniče Museum	Adult	6	Small areas on the inside of the both medial orbital plates, distal portion of the right temporal area	Dacrion left and right, sphenion right	14
Podkumok	Russia	Moscow University Museum of Anthropology, Moscow, Russia	Adult	6	Distal parts of the temporal areas; medial part of the left orbit	Sphenion left and right, dacrion left, maxillofrontale left	8
Předmostí 3[a]	Czech Republic	Dolni Vestoniče Museum	Adult	6	Distal temporal region on the left; lateral areas of the nasal region on both sides	Dacrion right, maxillofrontle left and right	3

TABLE 1. Fossils sample (Continued)

Name	Origin	Collection	Dental age	Dental stage	Reconstruction		
					Areas	Landmarks	Total landmarks and outline semilandmarks
Qafzeh 1[a]	Israel	Musee de l'Homme, Paris	Adult	6	Distal left temporal area	Sphenion left	5
Qafzeh 2[a]	Israel	Musee de l'Homme, Paris	Adult	6	Distal left temporal area and the inside portion of the medial orbital plate on the right	Sphenion right, dacrion right	5
Skhodnya	Russia	Moscow University Museum of Anthropology, Moscow, Russia	Adult	6	Medial portion of the right orbit; distal parts of both temporal areas	Sphenion left and right, dacrion right, maxillofrontale right	14
Sungir' 1	Russia	Laboratory of reconstruction, Russian Academy of Science, Moscow	Adult	6	None	None	None
Sungir' 2	Russia	Laboratory of reconstruction, Russian Academy of Science, Moscow	13	5	None	None	None
Sungir' 3	Russia	Laboratory of reconstruction, Russian Academy of Science, Moscow	9	4	None	None	None
Neanderthals							
Amud 1	Israel	Dept. of Anatomy and Anthropology, Tel Aviv University	Adult	6	Medial portions of both orbital rims and distal end of the right temporal area	Sphenion right, dacrion left and right, maxillofrontale right	6
La Chapelle-aux-Saints	France	Musee de l'Homme, Paris	Adult	6	Small area at the posterior portion of the frontal squama on the left	None	8
La Ferrassie 1	France	Musee de l'Homme, Paris	Adult	6	Posterior portion of the frontal squama on the right; small distal part of the left temporal region; distal part of the right zygomatic process	Stephanion right, sphenion right, dacrion right, frontomalare anterior right, frontomalare orbitale right, frontomalare temporale right, maxillofrontale left	18
La Quina H5	France	Musee de l'Homme, Paris	Adult	6	Nasal area; left temporal area	Nasion, sphenion left, dacrion left and right, maxillofrontale left and right	13
Šal'a 1	Slovak Republic	Slovenske Narodne Muzeum, Bratislava	Adult	6	None	None	None
Shanidar 1[a]	Iraq	Musee de l'Homme, Paris	Adult	6	Left temporal region and medial portion of the left orbit	Sphenion left, dacrion right, frontomalare anterior left, maxillofrontale left	6
Spy 1	Belgium	NESPOS CT scan data	Adult	6	Medial and lateral areas of the right orbit, maxillofrontale area on the left	Dacrion left, dacrion right, frontomalare anterior right, frontomalare orbitale right, frontomalare temporale right, maxillofrontale left	8

TABLE 1. Fossils sample (Continued)

Name	Origin	Collection	Dental age	Dental stage	Reconstruction		
					Areas	Landmarks	Total landmarks and outline semilandmarks
Spy 2	Belgium	NESPOS CT scan data	Adult	6	Nasal area, maxillofrontal areas on both sides, outline of the fronto-sphenoidal suture on both sides	Glabella, nasion, sphenion right, dacrion left, dacrion right, frontomalare anterior left, frontomalare anterior right, frontomalare orbitale left frontomalare orbitale right, frontomalare temporale right, maxillofrontale left, maxillofrontale right	18
Gibraltar 1	Gibraltar	Natural History Museum, London	Adult	6	About quarter of the posterior surface of the frontal squama on the left side spanning over bregma; small distal end of the left zygomatic process. Reconstructed by reflection.	Bregma, stephanion left, frontotemporale left, sphenion left, frontomalate anterior left, frontomalare orbitale left, frontomalare temporale left	After reflection—11
Feldhofer 1	Germany	Rheinisches Landesmuseum, Bonn	Adult	6	Small area around frontotemporale right	Frontotemporale right	3
Pech de L'Azé	France	Musee de l'Homme, Paris	3	3	Small area on the inside of the left medial orbital plate	Dacrion left	1
Engis	Belgium	University of Liege, Liege	4.5[b]	3	A large area of the left part of the frontal is absent; the reconstruction was performed by means of reflection of the right part	Stephanion left, frontotemporale left, sphenion left, frontomalare anterior left, frontomalare orbitale left, frontomalare temporale left	After reflection—2
Gibraltar 2	Gibraltar	Natural History Museum, London	4	3	Small area on the inside of the right medial orbital plate; distal ends of both zygomatic processes	Dacrion right, frontomalare anterior left and right, frontomalare orbitale left and right, frontomalare temporale left and right	8
Le Moustier 1	France	Museum für Vor- and Fruhgeschichte, Berlin	15	5	Distal part of the right zygomatic process; inside of the right medial orbital plate spanning over to the nasal area but not to nasion	Dacrion right, frontomalare anterior right, frontomalare orbitale right, frontomalare temporale right, maxillofrontale right	13
Early modern humans							
Qafzeh 6[a]	Israel	Musee de l'Homme, Paris	Adult	6	Distal right temporal area and the inside portion of the medial orbital plates on both sides	Sphenion right	8
Qafzeh 9	Israel	Department of Anatomy and Anthropology, Tel Aviv University	Adult	6	Nasal area, dacrion area on the left, lateral orbital rim on the left, fronto-sphenoidal suture on the left	Glabella, nasion, sphenion left, dacrion left, frontomalare anterior left	13

TABLE 1. Fossils sample (Continued)

Name	Origin	Collection	Dental age	Dental stage	Reconstruction		
					Areas	Landmarks	Total landmarks and outline semilandmarks
Qafzeh 10	Israel	Department of Anatomy and Anthropology, Tel Aviv University	6	4	Dacrion areas on both sides, left distal orbital rim, maxillofrontal area on the right	Dacrion left, dacrion right, frontomalare anterior left, frontomalare orbitale left, maxillofrontale right	9
Qafzeh 11	Israel	Department of Anatomy and Anthropology, Tel Aviv University	Adult	6	Left dacrion area, right zygomatic process	Dacrion left, frontomalare anterior right, frontomalare orbitale right, frontomalare temporale right	9
Skhul 1	Israel	Department of Anatomy and Anthropology, Tel Aviv University	5 (on mandible)	3	Area to the lateral and including right temporal line, right zygomatic process; reconstruction is done by reflection	Glabella nasion	after reflection—2
Skhul 5[a]	Israel	University College London, Anthropology Department	Adult	6	Medial portion of the left orbit; glabella, distal end of the left zygomatic process and distal part of the left temporal area	Sphenion left, dacrion left, frontomalare anterior left, frontomalare orbitale left, frontomalare temporale left	20
Unclassified							
Kabwe	Zambia	Natural History Museum, London	Adult	6	None	None	None
Satanay	Russia	Moscow University Museum of Anthropology, Moscow, Russia	Adult	6	none	None	None
Zuttiyeh[a]	Israel	Musee de l'Homme, Paris	Adult	6	Medial portion of the left orbit including maxillofrontale and an inside aspect of the right orbital plate	Dacrion left and right, maxillofrontale left	9
Teshik-Tash	Uzbekistan	Moscow University Museum of Anthropology, Moscow, Russia	9	4	None	None	None

[a] Measurements were taken on casts.
[b] Schwartz et al., 2002; Schwartz and Tattersall, 2003.

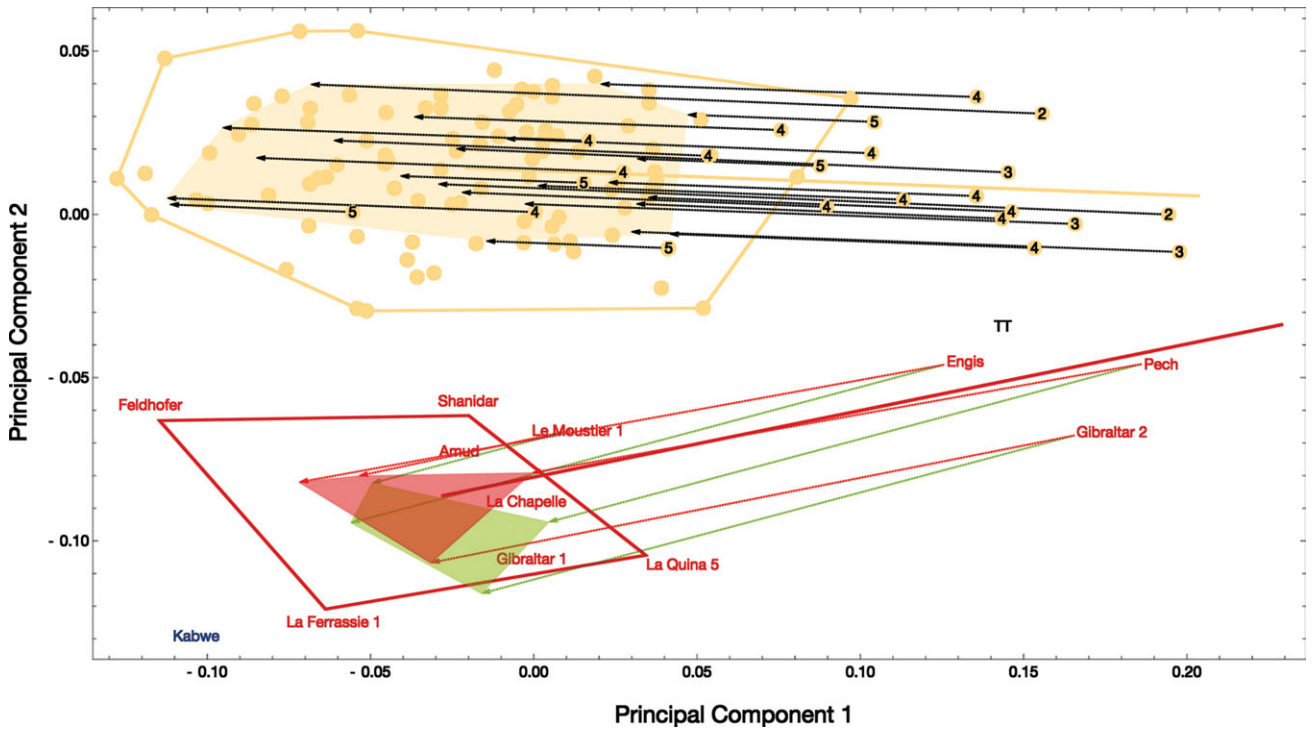

Fig. 2. Principal components (PC) 1 vs. 2 of shape space. Modern humans are in beige; Neanderthals in red. Subadult modern humans are labeled with their dental stages; adult convex hulls are drawn as outlines. For each subadult we predicted an adult shape based on regressions of shape on dental stage. Thick lines are the species regressions; the thin lines are the estimated developmental trajectories. Convex hulls for the simulated adult shapes are plotted as polygons, which are filled in the color of the developmental model used for prediction—red: Neanderthal regression model, green: early modern human regression model.

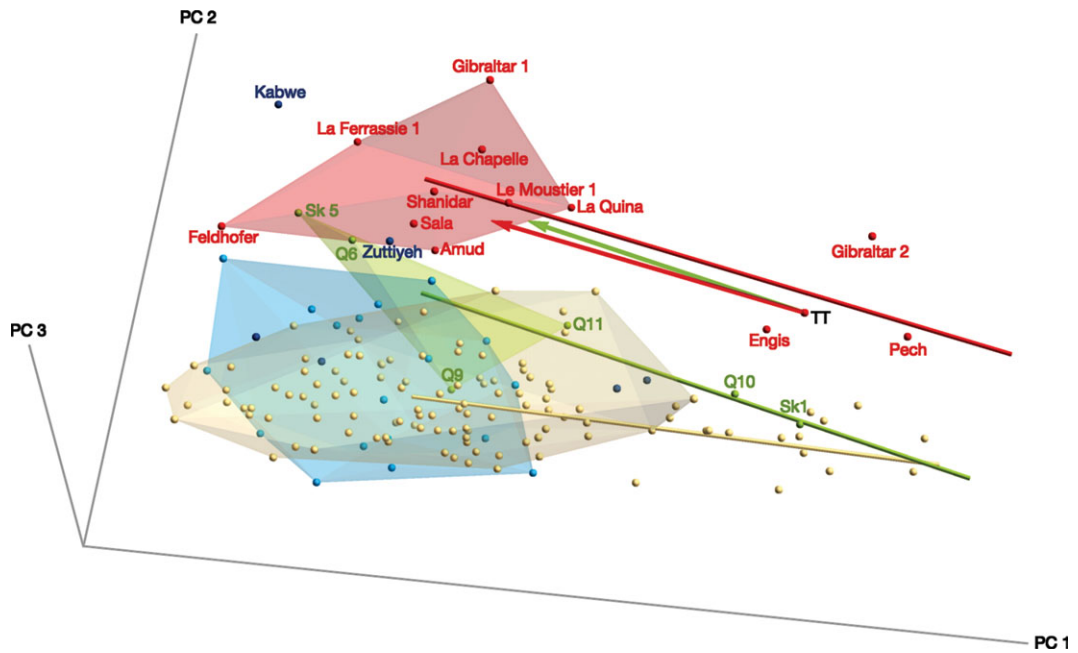

Fig. 3. First three PCs of shape space. Modern humans are in beige; Neanderthals in red. Subadult modern humans are labeled with their dental stages; convex hulls are drawn for the adult specimens of modern humans (beige), Neanderthals (red), early modern humans (green), Upper Paleolithic modern humans (blue). Linear regressions of shape on dental stage are drawn in the respective group color. Two developmental simulations based on the developmental patterns of early modern humans (green arrow) and Neanderthals (red arrow) predict adult shapes of Teshik-Tash that fall close to Neanderthal adults.

2009): surface semilandmarks were measured on a template specimen, then warped to every specimen based on a thin-plate spline interpolation computed from the landmarks and curve-semilandmarks. These warped points were then projected onto the surface. Subsequently, all 215 semilandmarks were allowed to slide on the surface, or the respective curves so as to minimize the bending energy between each specimen and the Procrustes mean shape. This sliding step establishes geometric homology among semilandmarks by removing the effect of the arbitrary semilandmark spacing from the coordinate data (Bookstein, 1997; Bookstein et al., 1999); the slid semilandmarks and landmarks can be treated the same in statistical analyses. Algebraic details of the semilandmark sliding algorithm can be found in Gunz et al. (2005).

Missing data estimation

A number of fossil specimens required the reconstruction of missing coordinates (listed in Table 1). We followed the geometric morphometrics reconstruction protocol developed by Gunz et al. (2009). Landmarks or semilandmarks missing on only one side of the frontal bone were estimated by mirror-imaging, based on the available paired landmarks and the symmetry axis defined by the midsagittal curve. Landmarks and semilandmarks missing on both sides or along the midsagittal, were estimated based on the thin-plate spline algorithm during the semilandmark sliding process (Gunz et al., 2009, 2012; Grine et al., 2010; Neubauer et al., 2012b; Weber et al., 2012): missing landmarks or semilandmarks were allowed to move so as to minimize the bending energy between each incomplete specimen and the sample Procrustes average shape. As many fossils were reconstructed by mirror-imaging one side, we subsequently symmetrized (Supporting Information Fig. 1) all individuals in the dataset using reflected relabeling (Mardia et al., 2000; Gunz et al., 2009). For data processing and analyses we used Mathematica (Wolfram Research).

To assess the error of this reconstruction method, we simulated the reconstruction of the two least complete fossils in our sample (i.e. the largest number of missing landmarks), Skhūl V and Mladeč 2. In the first simulation we deleted the same landmarks and semilandmarks missing in Skhūl V from each recent modern human adult, and compared the reconstruction to the original. In the second simulation we deleted the landmarks and semilandmarks missing in Mladeč 2, from Teshik-Tash, and compared the reconstructed shape to the original shape.

Statistical analyses

The 3D coordinates of landmarks and slid semilandmarks were converted to shape variables by Procrustes superimposition (Rohlf and Slice, 1990; Dryden and Mardia, 1998). Centroid size was calculated as the square root of the sum of squared distances from each landmark to the specimen's centroid. We assessed large-scale trends in the data using principal component analysis (PCA) computed from the covariance matrix of the Procrustes shape coordinates.

Developmental trajectories were calculated for Neanderthals (NEA), early modern humans (EMH) and recent modern humans (RMH) based on dental stages. All individuals were assigned a dental development stage: stage 1—no teeth erupted, stage 2—incomplete deciduous dentition; 3—complete deciduous dentition, 4—M1 erupted; 5—M2 erupted; 6—M3 erupted (adult). Fossil specimens that did not have any teeth preserved were assigned to a group in accordance with their published biological age (Schwartz et al., 2002; Schwartz and Tattersall, 2003). We then calculated a linear regression of Procrustes shape variables on dental developmental stage for each group separately.

Subsequently, we used developmental simulations (McNulty et al., 2006; Singleton et al., 2010; Neubauer et al., 2010; Gunz et al., 2010, 2012; Gunz, 2012) to predict adult shapes for Teshik-Tash. Such developmental simulations can be computed based on size (Gunz, 2012), dental stage via shape differences between group means (Neubauer et al., 2010; Gunz et al., 2012), or dental stage via regression (McNulty et al., 2006). Here we used the dental stage via regression approach (see Discussion below). To this end we added multiples of the coefficients (slopes) from the linear regressions of early modern humans and Neanderthals, respectively, to the Procrustes shape coordinates of Teshik-Tash to predict shapes at dental stage 6 (McNulty et al., 2006). No developmental simulations were computed for the Upper Paleolithic (UP) specimens, because the small subadult sample size (only Sungir' 2 and 3 are subadults, at dental stages 5 and 4, respectively) makes the estimation of the UP developmental trajectory unreliable (Gunz, 2012).

To validate our method of simulating developmental shape changes, we predicted adult shapes for each modern human and Neanderthal subadult. For these simulations we used a jackknifing approach: each subadult was "grown" along a trajectory that was computed without it. We then projected these simulated adults into the Procrustes shape space of the original sample, to test whether they fell within the respective adult variation of Neanderthals and modern humans.

To assess the phenetic affinities of Teshik-Tash we used two approaches. First, we computed pairwise Procrustes distances to find the nearest neighbors in shape space for Teshik-Tash, and for the two simulated adult shapes of Teshik-Tash (one based on the Neanderthal developmental pattern, one on the early modern human developmental pattern, respectively). For the two simulated adult shapes we also computed log-likelihood ratios (Weber et al., 2006; Hublin et al., 2009) to classify them into one of three predefined groups: adult Neanderthals, adult early modern humans, and adult Upper Paleolithic modern humans. As the computation of the log-likelihood ratios requires full-rank group covariance matrices (i.e., more cases than variables), we used principal component analysis as a dimension reduction technique. With four adult specimens, the early modern human sample was the smallest group; we therefore computed the log-likelihood ratios in the subspace of the first three principal components (i.e., $N_{\text{smallest group}} - 1$).

We used permutation tests (Good, 2005), based on the variance explained by the regression model, to assess the statistical significance of the multivariate regression of the Procrustes shape coordinates on dental stage, and the natural logarithm of centroid size (Mitteroecker et al., 2005).

We also used permutation statistics to test whether the developmental trajectories of recent modern humans, early modern humans and Neanderthals are parallel or diverging: we first subtracted the respective group mean

from each specimen. We then computed angles between regression-vectors of the Procrustes shape coordinates on dental stage. To test whether the angle between two vectors was significantly different from zero, we compared the actual angle with angles obtained from regressions computed for 10,000 permutations for which group memberships were reassigned (Gunz, 2012). A nonsignificant result implies that the null-hypothesis, that two vectors are identical or parallel, cannot be refuted.

RESULTS

Testing the method

We first tested our method of computing developmental simulations based on dental stages by predicting adult shapes for all Neanderthal and recent modern human subadults. In shape space all simulated adult shapes fall within the ranges of variation of the actual adults. Figure 2 shows the first two principal components (PCs) of shape space (which explain 58 and 13% of the total variance, respectively); the adult convex hulls for recent modern humans (beige), and Neanderthals are drawn as outlines. Convex hulls for the simulated adult shapes are plotted as polygons, which are filled in the color of the developmental model used for prediction—red: Neanderthal regression model, green: early modern human regression model.

Missing data estimation

When we simulated the estimation of the landmarks and semilandmarks missing in Skhūl V in our adult recent modern human sample, the reconstruction error (measured as the average distance between the reconstructed and original positions of landmarks and semilandmarks) was <1 mm (0.97 mm ± 0.69 S.D.). The shape differences between original and reconstruction were negligible: in PC space, the original and reconstructed shapes overlap (Supporting Information Fig. 2A). Likewise, the reconstruction error was negligible when we reconstructed those landmarks and semilandmarks missing in Mladeč 2 from the complete frontal of Teshik-Tash (Supporting Information Fig. 2).

Principal component analysis

Figure 3 shows the first three PCs in shape space (the total variance explained by the first three PCs is ~76%). Here, the filled convex hulls represent the actual adult Neanderthals (red), recent modern humans (beige), early modern humans (green), and Upper Paleolithic modern humans (blue). Recent modern humans and Neanderthals are separated in shape space, throughout development (Figs. 2 and 3). Upper Paleolithic frontal bones either fall within or close to the adult variation of recent modern humans. In the space of the first three PCs early modern human fossils from Skhūl and Qafzeh plot in between modern humans and Neanderthals.

Regressions on dental stage

The regressions of Procrustes shape on dental stage are drawn as lines in the respective group color. These lines do seem to diverge (in the space of the first three PCs the angles are: 13.4° between recent modern humans and Neanderthals, 18° between early modern humans and recent modern humans, 4° between early modern humans and Neanderthals). However, these angular differences are not statistically different from zero, neither in the subspace of the first three PCs, nor in full shape space.

We also tested the significance of the regressions of frontal bone shape on dental stage, based on the explained variance. Among Neanderthals dental stage accounts for 60% of the shape variance ($P < 0.0004$), among early modern humans dental stage accounts for 55% of the shape variance ($P < 0.017$), and among recent modern humans for 36.7% ($P < 0.002$).

Regressions on size

Regressions of frontal bone shape on the natural logarithm of centroid size (i.e., ontogenetic allometry) explain 32% of the total shape variance among Neanderthals ($P < 0.02$), and only 6% among recent modern humans ($P < 0.0013$). The explained variance is 43% among early modern humans; however, this value is not statistically significant ($P < 0.076$). Allometry explains only 2.9% of the shape variance among Upper Paleolithic specimens; this value is not statistically significant ($P < 0.77$).

Developmental simulations

The two developmental simulations of Teshik-Tash are drawn as arrows in Figure 3; red for the adult prediction based on the Neanderthal developmental pattern, green for the adult prediction based on the early modern human pattern. It is evident that both adult shapes plot close to Neanderthal adults. We visualized the predicted shape changes in Figure 4 and Supporting Information Figure 3. It is evident from these simulations that the frontal bone shape of the Teshik-Tash child would have changed considerably, if it had reached adulthood. The temporal lines would have moved superiorly, the supraorbital torus would have become more projecting, and the cranial vault would have become much lower. In Figure 4 we used the landmarks and semilandmarks shown in Supporting Information Figure 3A to warp a surface scan of a Teshik-Tash cast using the thin-plate spline interpolation function (Gunz et al., 2005; Gunz and Harvati, 2007). The predicted ontogenetic shape changes of the frontal bone are quite pronounced, and the resemblance of the predicted adult shape of Teshik-Tash to Neanderthal adults is striking.

Phenetic affinities

In the space of the first three principal components of shape space (Figs. 2 and 3) Teshik-Tash plots closest to the Neanderthal subadult from Engis; base on pairwise Procrustes distances, that take all dimensions of shape space into account, the nearest neighbor of Teshik-Tash is the Neanderthal subadult Gibraltar 2. For both simulated adult shapes of Teshik-Tash, the respective nearest neighbor in shape space is the Neanderthal from La Chapelle aux Saints.

Log-likelihood ratios for both simulated adult shapes of Teshik-Tash consistently classified them as Neanderthals. The adult shape predicted based on the early modern human developmental pattern is 36 times more likely to be a Neanderthal than an Upper Paleolithic modern human, and 3,127 times more likely to be a Neanderthal than an early modern human fossil. When we use the Neanderthal developmental pattern to predict an adult shape of Teshik-Tash, its morphology is 11 times more likely to be a Neanderthal than an Upper Paleo-

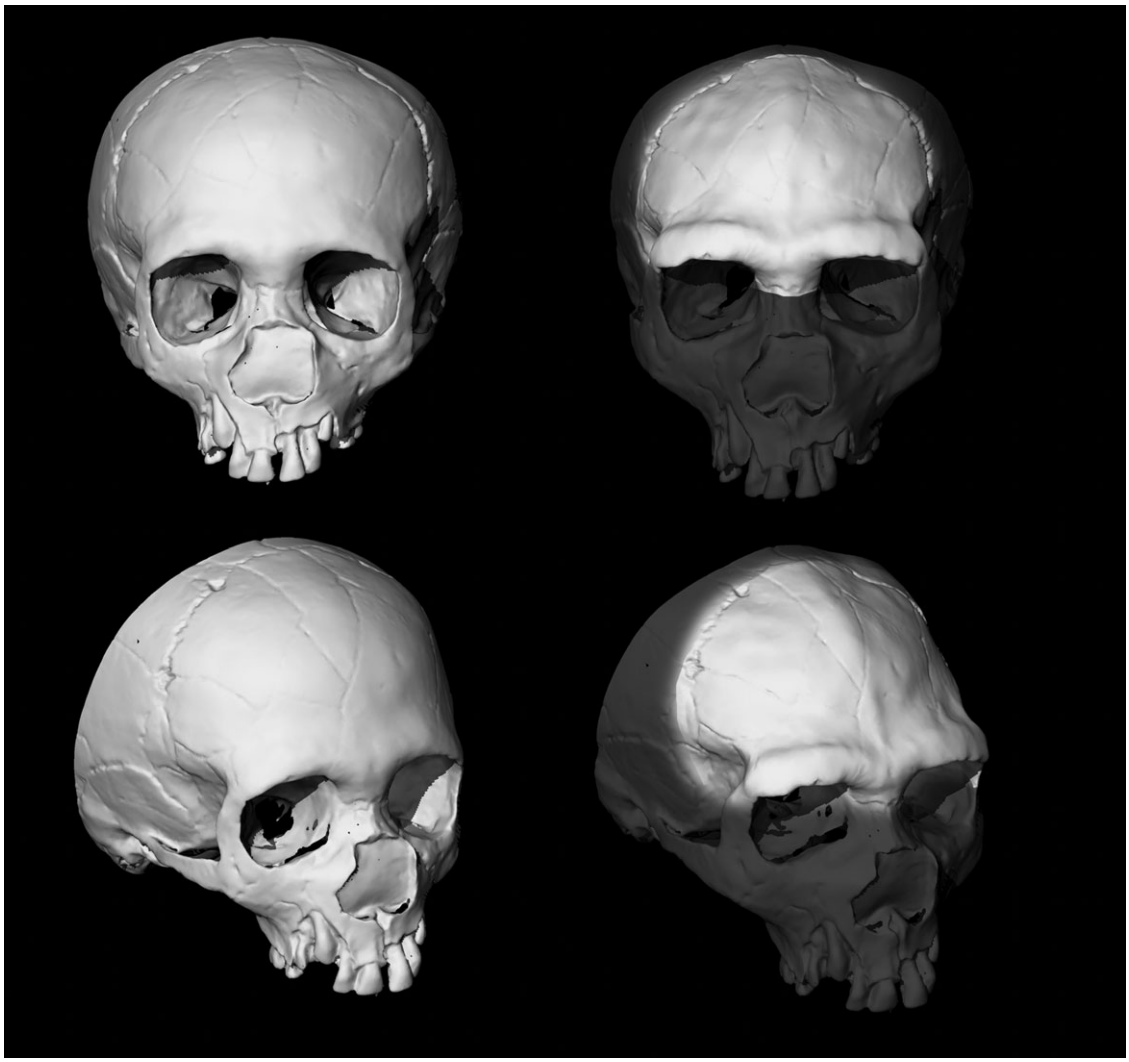

Fig. 4. Simulated adult shape of Teshik-Tash based on the Neanderthal developmental pattern. A surface scan of a Teshik-Tash cast (left) was warped according to the landmarks and semilandmarks in Supporting Information Figure 3 (right). Areas between measurements are interpolated based on the thin-plate spline interpolation function.

lithic modern human, and 16,623 times more likely to be a Neanderthal than an early modern human fossil.

DISCUSSION

The aim of our article was to assess the phenetic affinities of the frontal bone of the Teshik-Tash hominin in light of ontogenetic shape changes. Our results conclusively classify the Teshik-Tash frontal bone morphology as a Neanderthal. With regard to frontal bone shape Teshik-Tash is closest to Gibraltar 2, a subadult Neanderthal, which is considerably younger in ontogenetic age than Teshik-Tash (Tillier, 1982; Dean et al., 1986; Skinner, 1997).

Our developmental simulations among modern humans and Neanderthals show that linear regressions of shape on dental stage provide a reliable way of estimating ontogenetic shape changes of frontal bone morphology. By contrast, linear regressions of shape on the natural logarithm of centroid size explained substantially less of the shape variance (59.7% dental stage vs. 26.6% size in Neanderthals, and 36.7% vs. 6% in recent modern humans). As mentioned above, neurocranial size is not a reliable proxy for development in the later stages of ontogeny, because the adult size of the brain is attained much earlier than adult facial size. The pronounced ontogenetic shape changes of the frontal bone's external morphology have very little impact on its overall size. To model the ontogenetic shape changes of the frontal bone during later ontogeny (i.e., after adult brain size has been achieved), predictions based on dental stage are therefore more appropriate than predictions based on size.

The estimation of missing data has a negligible effect on the analysis (Supporting Information Figs. 1 and 2). When we simulate the reconstruction of the two most affected cases Skhūl V and Mladeč 2 using complete specimens, the resulting reconstructions are almost identical to the originals. Our TPS estimates of missing data are computed based on the mean shape of the entire sample. This mean shape is biased toward the largest group in the sample, i.e., recent modern humans. If there is any bias, our reconstruction method is therefore biased against our finding, as it makes incomplete fossils

appear to be more recent, modern, and human-like (Gunz et al., 2009).

The developmental patterns of early modern humans and Neanderthals are very similar. Whereas the developmental trajectories do not appear to be parallel in Figures 2 and 3, the angles between the trajectories are not statistically significant from zero. We therefore cannot reject the hypothesis that the developmental trajectories are parallel. Given the small number of fossils, this nonsignificant result might be attributed to the small sample sizes, in particular to the small subadult sample. Our developmental simulations based on Neanderthals and early modern humans (Figs. 2–4), however, clearly indicate that the developmental patterns of the frontal bone are almost identical between Neanderthals and early modern humans, regardless of the level of significance. This result is consistent with previous studies on hominin craniofacial development that have reported extremely conserved developmental patterns after the eruption of the first permanent molar (Ponce de León and Zollikofer, 2001; Ackermann and Krovitz, 2002; Williams et al., 2002a, 2002b; Bookstein et al., 2003; Bastir and Rosas, 2004a,b; Cobb and O'Higgins, 2004; Mitteroecker et al., 2004a,b; Schaefer et al., 2004; Zollikofer and Ponce De León, 2004; Mitteroecker et al., 2005, 2012; McNulty et al., 2006; Bulygina et al., 2006; Ponce de León and Zollikofer, 2006; Bastir et al., 2007; Cobb and O'Higgins, 2007; Lieberman et al., 2007; Mitteroecker and Bookstein, 2008; Neubauer et al., 2009).

The position of the early modern humans from Skhūl and Qafzeh (Fig. 3) "in-between" recent modern humans and Neanderthals has been documented in previous analyses (for example McCown and Keith, 1939; Stringer and Andrews, 1988; Simmons and Smith, 1991a,b; Simmons et al., 1991; Weber et al., 2006; Harvati et al., 2007; Schillaci, 2008; Gunz et al., 2009; Athreya, 2009; Harvati, 2009; Harvati et al., 2010; Stansfield Nee Bulygina and Gunz, 2011; Freidline et al., 2012).

In both developmental simulations, the simulated adult shapes are closest to the Neanderthal from La Chapelle aux Saints. This consistency is another indication that the developmental patterns of Neanderthals and early modern humans are very similar. Moreover, the log-likelihood ratios always classify the two simulated adult shapes of Teshik-Tash as Neanderthal adults: even when we use the early modern human developmental pattern to simulate the adult shape of Teshik-Tash, this simulated adult is still more than 3,000 times more likely to be a Neanderthal than an early modern human adult. When we use the Neanderthal developmental pattern to "grow" Teshik-Tash, it is >16,000 times more likely to be a Neanderthal than an early modern human. The statistical evidence in the comparison Upper Paleolithic modern human or Neanderthal is also unequivocal, although interestingly the numbers are significantly smaller: both simulated adult shapes of Teshik-Tash are more likely to be a Neanderthal than an Upper Paleolithic modern human—21 times and 8.5 times, respectively.

In summary, all of our analyses consistently classify Teshik-Tash as a Neanderthal. The difference between the results reported here, and those by Glantz et al. (2009) are most likely related to different sample compositions, as well as to methodological differences. The current study focused on the details of frontal bone morphology, as this area is well preserved in Teshik-Tash and many other relevant fossils, whereas Glantz et al. (2009) analyzed measurements from the unreconstructed parts of the entire cranium and the mandible. Here we used developmental simulations to predict the adult morphology of Teshik-Tash based on regressions of shape on dental stage. We do not consider our analysis a formal test of the finding of Glantz et al. (2009), as the sample compositions are different, and our study focused on the frontal bone. Future studies should assess the phenetic affinities of the Teshik-Tash skull beyond the frontal bone morphology, however taking into consideration that aspects of its morphology were reconstructed, as well as the subadult status of the specimen.

In agreement with the findings of Glantz et al. (2009) our log-likelihood ratios find the frontal bone of Teshik-Tash to be more similar to Upper Paleolithic humans than to the early modern humans from Skhūl and Qafzeh, contradicting Weidenreich (1945). Recent modern humans and Upper Paleolithic modern humans overlap, but there is no overlap with Neanderthals (Fig. 3). The frontal bone of Teshik-Tash is clearly Neanderthal-like when analyzed in the framework of developmental shape changes.

CONCLUSIONS

The morphology of the frontal bone places the Teshik-Tash child close to other Neanderthal children; the simulated adults are closest to Neanderthal adults. Taken together with a recent genetic analysis, which showed that Teshik-Tash carried mtDNA of the Neanderthal type (Krause et al., 2007), its occipital bun, and its shovel-shaped upper incisors, these independent lines of evidence firmly place Teshik-Tash among Neanderthals.

ACKNOWLEDGMENTS

The authors are most grateful to the people who allowed the work with the original fossil and modern material in their care: Vladimir Chtetsov, Vitaliy Kharitonov, and Denis Pezhemski from the Anthropology Museum of the Moscow State University; Tatiana Balueva from the Laboratory of Reconstruction, Institute of Anthropology and Ethnology, Russian Academy of Science; Robert Kruzinski and Louise Humphrey from the Natural History Museum, London; Philippe Mennecier, Musee de l'Homme, Paris; Maria Teschler-Nicola, Natural History Museum in Vienna; Maggie Belatti and Martha Lahr, Leverhulme Center for Human Evolutionary Studies, Cambridge; Jirí Svoboda, Archeological Museum in Dolní Věstonice; Alena Sefčakova, Slovenske Narodne Muzeum, Bratislava; Edouard Poty, University of Liege; Michael Schmauder, Rheinisches Landesmuseum, Bonn; and Almut Hoffmann, Museum für Vor- und Frühgeschichte, Berlin. They are grateful to Alyson Reid for proofreading the text. The constructive criticism of Mica Glantz, Sheela Athreya, and Terrence Ritzman, as well as Chris Ruff and two anonymous referees helped to improve the manuscript.

LITERATURE CITED

Ackermann RR, Krovitz GE. 2002. Common patterns of facial ontogeny in the hominid lineage. Anat Rec 269:142–147.

Athreya S. 2006. Patterning of geographic variation in Middle Pleistocene *Homo* frontal bone morphology. J Hum Evol 50:627–643.

Athreya S. 2009. A comparative study of frontal bone morphology among Pleistocene hominin fossil groups. J Hum Evol 57:786–804.

Bailey S, Glantz M, Weaver TD, Viola B. 2008. The affinity of the dental remains from Obi-Rakhmat Grotto, Uzbekistan. J Hum Evol 55:238–248.

Bastir M, Rosas A. 2004a. Comparative ontogeny in humans and chimpanzees: similarities, differences and paradoxes in postnatal growth and development of the skull. Ann Anat 186:503–509.

Bastir M, Rosas A. 2004b. Facial heights: evolutionary relevance of postnatal ontogeny for facial orientation and skull morphology in humans and chimpanzees. J Hum Evol 47:359–381.

Bastir M, O'Higgins P, Rosas A. 2007. Facial ontogeny in Neanderthals and modern humans. Proc Biol Sci 274:1125–1132.

Bayle P, Braga J, Mazurier A, Macchiarelli R. 2009. Dental developmental pattern of the Neanderthal child from Roc de Marsal: a high-resolution 3D analysis. J Hum Evol 56:66–75.

Bayle P, Macchiarelli R, Trinkaus E, Duarte C, Mazurier A, Zilhão J. 2010. Dental maturational sequence and dental tissue proportions in the early Upper Paleolithic child from Abrigo do Lagar Velho, Portugal. Proc Natl Acad Sci USA 107:1338–1342.

Bookstein FL. 1991. Morphometric tools for landmark data: geometry and biology. Cambridge: Cambridge University Press.

Bookstein FL. 1997. Landmark methods for forms without landmarks: morphometrics of group differences in outline shape. Med Image Analysis 1:225–243.

Bookstein FL, Schäfer K, Prossinger H, Seidler H, Fieder M, Stringer C, Weber GW, Arsuaga J-L, Slice DE, Rohlf FJ, Recheis W, Mariam AJ, Marcus LF. 1999. Comparing frontal cranial profiles in archaic and modern *Homo* by morphometric analysis. Anat Rec 257:217–224.

Bookstein FL, Gunz P, Mitteroecker P, Prossinger H, Schaefer K, Seidler H. 2003. Cranial integration in *Homo*: singular warps analysis of the midsagittal plane in ontogeny and evolution. J Hum Evol 44:167–187.

Buikstra JE, Ubelaker DH. 1994. Proceedings of a seminar at the field museum of natural history. Standards for data collection from human skeletal remains. Fayetteville, AR: Arkansas Archeological Survey.

Bulygina E. 2007. A comparative study of frontal bone morphology of Late Pleistocene fossil hominins from the territory of the former Soviet Union. Ph.D. Thesis, University College London, United Kingdom.

Bulygina E, Mitteroecker P, Aiello L. 2006. Ontogeny of facial dimorphism and patterns of individual development within one human population. Am J Phys Anthropol 131:432–443.

Cobb SN, O'Higgins P. 2004. Hominins do not share a common postnatal facial ontogenetic shape trajectory. J Exp Zool B Mol Dev Evol 302:302–321.

Cobb SN, O'Higgins P. 2007. The ontogeny of sexual dimorphism in the facial skeleton of the African apes. J Hum Evol 53:176–190.

Coqueugniot H, Hublin J-J. 2007. Endocranial volume and brain growth in immature Neandertals. Periodicum Biol 109:379.

Coqueugniot H, Hublin J-J. 2012. Growth of digital endocranial volumes in early human ontogeny: results from a reference osteological collection. Am J Phys Anthropol, in press.

Coqueugniot H, Hublin J-J, Veillon F, Houët F, Jacob T. 2004. Early brain growth in *Homo erectus* and implications for cognitive ability. Nature 431:299–302.

Cunningham DJ. 1908. The evolution of the eyebrow region of the forehead, with special reference to the excessive supraorbital development in the Neanderthal race. Trans R Soc Edinb 46:243–310.

Dean MC, Stringer CB, Bromage TG. 1986. Age at death of the Neanderthal child from Devil's Tower, Gibraltar and the implications for studies of general growth and development in Neanderthals. Am J Phys Anthropol 70:301–309.

DeSilva JM, Lesnik JJ. 2008. Brain size at birth throughout human evolution: a new method for estimating neonatal brain size in hominins. J Hum Evol 55:1064–1074.

Di Vincenzo F, Churchill SE, Manzi G. 2012. The Vindija Neanderthal scapular glenoid fossa: comparative shape analysis suggests evo-devo changes among Neanderthals. J Hum Evol 62:274–285.

Dryden IL, Mardia KV. 1998. Statistical shape analysis. Chichester: Wiley.

Freidline SE, Gunz P, Janković I, Harvati K, Hublin J-J. 2012. A comprehensive morphometric analysis of the frontal and zygomatic bone of the Zuttiyeh fossil from Israel. J Hum Evol 62:225–241.

Glantz MM. 2010. The history of hominin occupation of Central Asia in review. Asian Paleoanthropol 101–112.

Glantz MM, Athreya S, Ritzman T. 2009. Is Central Asia the eastern outpost of the Neandertal range? A reassessment of the Teshik-Tash child. Am J Phys Anthropol 138:45–61.

Glantz MM, Viola B, Chikisheva T. 2004. New hominid remains from Obi-Rakhmat grotto. Grot Obi-Rakhmat. Novosibirsk: Institute of Archeology and Ethnography, Siberian Branch, Russian Academy of Sciences. p77–93.

Glantz MM, Viola B, Wrinn P, Chikisheva T, Derevianko A, Krivoshapkin A, Islamov U, Suleimanov R, Ritzman T. 2008. New hominin remains from Uzbekistan. J Hum Evol 55:223–237.

Good PI. 2005. Permutation, parametric and bootstrap tests of hypotheses. New York: Springer.

Green RE, Krause J, Briggs AW, Maricic T, Stenzel U, Kircher M, Patterson N, Li H, Zhai W, Fritz MH, Hansen NF, Durand EY, Malaspinas AS, Jensen JD, Marques-Bonet T, Alkan C, Prüfer K, Meyer M, Burbano HA, Good JM, Schultz R, Aximu-Petri A, Butthof A, Höber B, Höffner B, Siegemund M, Weihmann A, Nusbaum C, Lander ES, Russ C, Novod N, Affourtit J, Egholm M, Verna C, Rudan P, Brajkovic D, Kucan Z, Gusic I, Doronichev VB, Golovanova LV, Lalueza-Fox C, de la Rasilla M, Fortea J, Rosas A, Schmitz RW, Johnson PL, Eichler EE, Falush D, Birney E, Mullikin JC, Slatkin M, Nielsen R, Kelso J, Lachmann M, Reich D, Pääbo S. 2010. A draft sequence of the Neandertal genome. Science 328:710–722.

Gremiatsky MA. 1949. The skull of the Neandertal child from the cave of Teshik-Tash, southern Uzbekistan. In: Gremiatsky MA, Nesturkh MF, editors. Teshik Tash: Paleolithic man. Moscow: Moscow State University. p137–182.

Grine FE, Gunz P, Betti-Nash L, Neubauer S, Morris AG. 2010. Reconstruction of the Late Pleistocene human skull from Hofmeyr, South Africa. J Hum Evol 59:1–15.

Guatelli-Steinberg D, Reid DJ, Bishop TA, Larsen CS. 2005. Anterior tooth growth periods in Neandertals were comparable to those of modern humans. Proc Natl Acad Sci USA 102:14197–14202.

Guihard-Costa AM, Ramírez Rozzi F. 2004. Growth of the human brain and skull slows down at about 2.5 years old. Comptes Rendus-Palevol 3:397–402.

Gunz P. 2012. Evolutionary relationships among robust and gracile australopiths: an "Evo-Devo" perspective. Evol Biol, in press.

Gunz P, Bookstein FL, Mitteroecker P, Stadlmayr A, Seidler H, Weber GW. 2009. Early modern human diversity suggests subdivided population structure and a complex out-of-Africa scenario. Proc Natl Acad Sci USA 106:6094–6098.

Gunz P, Harvati K. 2007. The Neanderthal "chignon": variation, integration, and homology. J Hum Evol 52:262–274.

Gunz P, Mitteroecker P, Bookstein FL. 2005. Semilandmarks in three dimensions. In: Slice DE, editor. Modern morphometrics in physical anthropology. New York: Kluwer Academic/Plenum Publishers. p73–98.

Gunz P, Mitteroecker P, Neubauer S, Weber GW, Bookstein FL. 2009. Principles for the virtual reconstruction of hominin crania. J Hum Evol 57:48–62.

Gunz P, Neubauer S, Golovanova L, Doronichev V, Maureille B, Hublin J-J. 2012. A uniquely modern human pattern of endocranial development. Insights from a new cranial reconstruction of the Neandertal newborn from Mezmaiskaya. J Hum Evol 62:300–313.

Gunz P, Neubauer S, Maureille B, Hublin J-J. 2010. Brain development after birth differs between Neanderthals and modern humans. Curr Biol 20:R921–R922.

Gunz P, Neubauer S, Maureille B, Hublin J-J. 2011. Virtual reconstruction of the Le Moustier 2 newborn skull. Implications for Neandertal ontogeny. PALEO 22:155–172.

Harvati K. 2009. Into Eurasia: a geometric morphometric reassessment of the Upper Cave (Zhoukoudian) specimens. J Hum Evol 57:751–762.

Harvati K, Gunz P, Grigorescu D. 2007. Cioclovina (Romania): affinities of an early modern European. J Hum Evol 53:732–746.

Harvati K, Hublin J-J, Gunz P. 2010. Evolution of Middle-Late Pleistocene human cranio-facial form: a 3-D approach. J Hum Evol 59:445–464.

Hublin J-J. 2009. Out of Africa: modern human origins special feature: the origin of Neandertals. Proc Natl Acad Sci USA 106:16022–16027.

Hublin J-J, Coqueugniot H. 2006. Absolute or proportional brain size: that is the question. A reply to Leigh's (2006) comments. J Hum Evol 50:109–113.

Hublin J-J, Weston D, Gunz P, Richards M, Roebroeks W, Glimmerveen J, Anthonis L. 2009. Out of the North Sea: the Zeeland Ridges Neandertal. J Hum Evol 57:777–785.

Humphrey LT. 1998. Growth patterns in the modern human skeleton. Am J Phys Anthropol 105:57–72.

Jelinek J, Dupree L, Gallus A, Gams H, Narr KJ, Poulianos AN, Sackett JR, Schott L, Suchy J, Yakimov VP. 1969. Neanderthal Man and *Homo sapiens* in Central and Eastern Europe. Curr Anthropol 10:475–503.

Kharitonov V. 2009. Age status of the Neanderthal child from Teshik-Tash in relation to its position within the Neanderthal clade. In: International conference "Man and its social and biological environment." p10–19.

Krause J, Fu Q, Good JM, Viola B, Shunkov MV, Derevianko AP, Pääbo S. 2010. The complete mitochondrial DNA genome of an unknown hominin from southern Siberia. Nature 464:894–897.

Krause J, Orlando L, Serre D, Viola B, Prüfer K, Richards MP, Hublin J-J, Hänni C, Derevianko AP, Pääbo S. 2007. Neanderthals in central Asia and Siberia. Nature 449:902–904.

Krovitz GE. 2003. Shape and growth differences between Neandertals and modern humans: grounds for a species-level distribution? Camb Stud Biol Evol Anthropol 37:320–342.

Lahr M, Wright RVS. 1996. The question of robusticity and the relationship between cranial size and shape in *Homo sapiens*. J Hum Evol 31:157–191.

Leigh SR. 2012. Brain size growth and life history in human evolution. Evol Biol, in press.

Lieberman DE, Carlo J, Ponce de León M, Zollikofer CP. 2007. A geometric morphometric analysis of heterochrony in the cranium of chimpanzees and bonobos. J Hum Evol 52:647–662.

Macchiarelli R, Bondioli L, Debénath A, Mazurier A, Tournepiche JF, Birch W, Dean MC. 2006. How Neanderthal molar teeth grew. Nature 444:748–751.

Mardia KV, Bookstein FL, Moreton IJ. 2000. Statistical assessment of bilateral symmetry of shapes. Biometrika 87:285–300.

McCown TD, Keith A. 1939. The Stone Age of Mount Carmel: the fossil human remains from the Levalloiso-Mousterian. Oxford: Clarendon Press.

McNulty KP, Frost SR, Strait DS. 2006. Examining affinities of the Taung child by developmental simulation. J Hum Evol 51:274–296.

Minugh-Purvis N. 1988. Patterns of craniofacial growth and development in Upper Pleistocene hominids. Ph.D. Thesis, University of Pennsylvania.

Mitteroecker P, Bookstein F. 2007. The conceptual and statistical relationship between modularity and morphological integration. Syst Biol 56:818–836.

Mitteroecker P, Bookstein F. 2008. The evolutionary role of modularity and integration in the hominoid cranium. Evolution 62:943–958.

Mitteroecker P, Bookstein F. 2009. The ontogenetic trajectory of the phenotypic covariance matrix, with examples from craniofacial shape in rats and humans. Evolution 63:727–737.

Mitteroecker P, Gunz P. 2009. Advances in geometric morphometrics. Evol Biol 36:235–247.

Mitteroecker P, Gunz P, Bernhard M, Schaefer K, Bookstein FL. 2004a. Comparison of cranial ontogenetic trajectories among great apes and humans. J Hum Evol 46:679–697.

Mitteroecker P, Gunz P, Bookstein FL. 2005. Heterochrony and geometric morphometrics: a comparison of cranial growth in *Pan paniscus* versus *Pan troglodytes*. Evol Dev 7:244–258.

Mitteroecker P, Gunz P, Neubauer S, Müller G. 2012. How to explore morphological integration in human evolution and development? Evol Biol, in press.

Mitteroecker P, Gunz P, Weber GW, Bookstein FL. 2004b. Regional dissociated heterochrony in multivariate analysis. Ann Anat 186:463–470.

Neubauer S, Gunz P, Hublin J-J. 2009. The pattern of endocranial ontogenetic shape changes in humans. J Anat 215:240–255.

Neubauer S, Gunz P, Hublin J-J. 2010. Endocranial shape changes during growth in chimpanzees and humans: a morphometric analysis of unique and shared aspects. J Hum Evol 59:555–566.

Neubauer S, Gunz P, Schwarz U, Hublin J-J, Boesch C. 2012a. Endocranial volumes in an ontogenetic sample of chimpanzees from the Tai Forest National Park, Ivory Coast. Am J Phys Anthropol 147.

Neubauer S, Gunz P, Weber GW, Hublin J-J. 2012b. Endocranial volume of *Australopithecus africanus*: new CT-based estimates and the effects of missing data and small sample size. J Hum Evol 62:498–510.

Neubauer S, Hublin J-J. 2012. The evolution of human brain development. Evol Biol, in press.

Okladnikov AP. 1949. Investigations of the Mousterian site and the Neanderthal burial at the Teshik-Tash grotto, South Uzbekistan (Central Asia). In: Gremiatsky MA, Nesturkh MF, editors. Teshik Tash: paleolithic man. Moscow: Moscow State University. p7–85.

Otte M. 2007. Arguments for population movement of anatomically modern humans from Central Asia to Europe. In: Mellars P, editor. Rethinking the human revolution: new behavioral and biological perspectives on the origin and dispersal of modern humans. Cambridge: McDonald Institute for Archeological Research. p359–366.

Ponce de León MS, Golovanova L, Doronichev V, Romanova G, Akazawa T, Kondo O, Ishida H, Zollikofer CPE. 2008. Neanderthal brain size at birth provides insights into the evolution of human life history. Proc Natl Acad Sci USA 105:13764–13768.

Ponce de León MS, Zollikofer CPE. 2001. Neanderthal cranial ontogeny and its implications for late hominid diversity. Nature 412:534–538.

Ponce de León MS, Zollikofer CPE. 2006. Neanderthals and modern humans—chimps and bonobos: similarities and differences in development and evolution. In: Harvati K, Harrison T, editors. Neanderthals revisited: new approaches and perspectives. Dordrecht: Springer. p71–88.

Rak Y, Kimbel WH, Hovers E. 1994. A Neandertal infant from Amud Cave, Israel. J Hum Evol 26:313–324.

Ramírez Rozzi FV, Bermudez De Castro JM. 2004. Surprisingly rapid growth in Neanderthals. Nature 428:936–939.

Ramírez Rozzi FV, Sardi M. 2007. Crown-formation time in Neandertal anterior teeth revisited. J Hum Evol 53:108–113.

Reich D, Green RE, Kircher M, Krause J, Patterson N, Durand EY, Viola B, Briggs AW, Stenzel U, Johnson PL, Maricic T, Good JM, Marques-Bonet T, Alkan C, Fu Q, Mallick S, Li H, Meyer M, Eichler EE, Stoneking M, Richards M, Talamo S, Shunkov MV, Derevianko AP, Hublin J-J, Kelso J, Slatkin M, Pääbo S. 2010. Genetic history of an archaic hominin group from Denisova Cave in Siberia. Nature 468:1053–1060.

Rohlf FJ, Slice D. 1990. Extensions of the Procrustes method for the optimal superimposition of landmarks. Syst Zool 39:40–59.

Rosas A. 2001. Occurrence of Neanderthal features in mandibles from the Atapuerca-SH site. Am J Phys Anthropol 114:74–91.

Ruff CB, Walker A, Trinkaus E. 1994. Postcranial robusticity in *Homo*. III: Ontogeny. Am J Phys Anthropol 93:35–54.

Schaefer K, Mitteroecker P, Gunz P, Bernhard M, Bookstein FL. 2004. Craniofacial sexual dimorphism patterns and allometry among extant hominids. Ann Anat 186:471–478.
Schwartz JH, Tattersall I, Holloway RL. 2002. The human fossil record. New York: Wiley-Liss.
Schwartz JT, Tattersall I. 2003. The human fossil record. New York: Wiley-Liss.
Schillaci MA. 2008. Human cranial diversity and evidence for an ancient lineage of modern humans. J Hum Evol 54:814–826.
Simmons T, Falsetti AB, Smith FH. 1991. Frontal bone morphometrics of southwest Asian Pleistocene hominids. J Hum Evol 20:249–269.
Simmons T, Smith FH. 1991a. Human population relationships in the late Pleistocene. Curr Anthropol 32:623–627.
Simmons T, Smith FH. 1991b. Human population relationships in the Late Pleistocene. Curr Anthropol 32:623–627.
Sinel'nikov NA, Gremiatsky MA. 1949. Bones of the skeleton of the Neanderthal child from the cave of Teshik-Tash, southern Uzbekistan. In: Gremiatsky MA, Nesturkh MF, editors. Teshik Tash: paleolithic man. Moscow: Moscow State University. p123–188.
Singleton M, McNulty KP, Frost SR, Soderberg J, Guthrie EH. 2010. Bringing up baby: developmental simulation of the adult cranial morphology of *Rungwecebus kipunji*. Anat Rec (Hoboken) 293:388–401.
Skinner M. 1997. Age at death of Gibraltar 2. J Hum Evol 32:469–470.
Slice DE. 2007. Geometric morphometrics. Annu Rev Anthropol 36:261–281.
Smith FH, Ranyard GC. 1980. Evolution of the supraorbital region in Upper Pleistocene fossil hominids from South-Central Europe. Am J Phys Anthropol 53:589–610.
Smith TM, Tafforeau P, Reid DJ, Grün R, Eggins S, Boutakiout M, Hublin J-J. 2007a. Earliest evidence of modern human life history in North African early *Homo sapiens*. Proc Natl Acad Sci USA 104:6128–6133.
Smith TM, Tafforeau P, Reid DJ, Pouech J, Lazzari V, Zermeno JP, Guatelli-Steinberg D, Olejniczak AJ, Hoffman A, Radovcic J, Makaremi M, Toussaint M, Stringer C, Hublin J-J. 2010. Dental evidence for ontogenetic differences between modern humans and Neanderthals. Proc Natl Acad Sci USA 107:20923–20928.
Smith TM, Toussaint M, Reid DJ, Olejniczak AJ, Hublin J-J. 2007b. Rapid dental development in a Middle Paleolithic Belgian Neanderthal. Proc Natl Acad Sci USA 104:20220–20225.
Stansfield E, Gunz P. 2011. Skhodnya, Khvalynsk, Satanay, and Podkumok calvariae: possible Upper Paleolithic hominins from European Russia. J Hum Evol 60:129–144.
Stefan VH, Trinkaus E. 1998. Discrete trait and dental morphometric affinities of the Tabun 2 mandible. J Hum Evol 34:443–468.
Stringer CB, Andrews P. 1988. Genetic and fossil evidence for the origin of modern humans. Science 239:1263–1268.
Stringer CB, Gamble C. 1993. In search of the Neanderthals. London: Thames and Hudson.
Tillier AM. 1982. Les enfants néanderthaliens de Devil's Tower (Gibraltar). Zeitschrift Morphol Anthropol 73:125–148.
Tillier AM. 1995. Neanderthal ontogeny: a new source for critical analysis. Anthropologie 33:63–68.
Tillier AM. 1996. The Pech de l'Azé and Roc de Marsal children (Middle Paleolithic, France): skeletal evidence for variation in Neanderthal ontogeny. Hum Evol 11:113–119.
Trinkaus E. 2003. Neandertal faces were not long: modern human faces are short. Proc Natl Acad Sci USA 100:8142–8145.
Trinkaus E, Athreya S, Churchill SE, Demeter F, Henneberg M, Kondo O, Manzi G, Maureille B, Trinkaus E. 2006. Modern human versus Neandertal evolutionary distinctiveness. Curr Anthropol 47:597–620.
Viðarsdóttir US, Cobb S. 2004. Inter- and intra-specific variation in the ontogeny of the hominoid facial skeleton: testing assumptions of ontogenetic variability. Ann Anat 186:423–428.
Viðarsdóttir US, O'Higgins P, Stringer C. 2002. A geometric morphometric study of regional differences in the ontogeny of the modern human facial skeleton. J Anat 201:211–229.
Viola B, Seidler H, zur Nedden D. 2004. Computer tomographic investigations of the OR-1 petrosals. In: Derevianko AP, editor. Grot Obi-Rakhmat. Novosibirsk: Institute of Archeology and Ethnography, Siberian Branch, Russian Academy of Sciences. p100–105.
Vlcek E. 1991. Fossil Man in Central-Europe. Anthropologie 95:409–472.
Weber GW, Gunz P, Mitteroecker A, Stadlmayr FL, Bookstein H, Seidler H. 2006. External geometry of Mladeč neurocrania compared with anatomically modern humans and Neanderthals. In: Teschler-Nicola M, editor. Early modern humans at the Moravian Gate: Mladeč Caves and their remains. New York: Springer. p453–471.
Weber GW, Gunz P, Neubauer S, Mitteroecker P, Bookstein FL. 2012. Digital South African fossils: morphological studies using reference-based reconstruction and electronic preparation. In: Reynolds SC, Gallagher A, editors. African genesis: perspectives on hominin evolution. Cambridge: Cambridge University Press. p298–316.
Weidenreich F. 1943. The "Neanderthal Man" and the ancestors of "*Homo sapiens*". Am Anthropol 45:39–48.
Weidenreich F. 1945. The Palaeolithic child from the Teshik-Tash Cave in southern Uzbekistan (Central Asia). Am J Phys Anthropol 3:151–163.
Williams FL. 2001. Heterochronic perturbations in the craniofacial evolution of *Homo* (Neandertals and modern humans) and *Pan* (*Pan troglodytes* and *P. paniscus*). PhD Thesis, University of Massachusetts, Amherst.
Williams FLE, Godfrey LR, Sutherland MR. 2002a. Diagnosing heterochronic perturbations in the craniofacial evolution of *Homo* (Neandertals and modern humans) and *Pan* (*P. troglodytes* and *P. paniscus*). In: Thompson JL, Krovitz GE, Nelson AJ, editors. Patterns of growth and development in the genus *Homo*. Cambridge: Cambridge University Press. p295–319.
Williams FLE, Godfrey LR, Sutherland MR. 2002b. Heterochrony and the evolution of Neandertal and modern human craniofacial form. In: Minugh-Purvis N, McNamara J, editors. Human evolution through developmental change. Baltimore: Johns Hopkins University Press. p405–441.
Williams FLE, Krovitz GE. 2004. Ontogenetic migration of the mental foramen in Neandertals and modern humans. J Hum Evol 47:199–219.
Wolpoff M, Mannheim B, Mann A, Hawks J, Caspari R, Rosenberg K, Frayer D, Gill K, Clark G. 2004. Why not the Neandertals? World Archeol 36:527–546.
Zollikofer CPE, Ponce De León MS. 2004. Kinematics of cranial ontogeny: heterotopy, heterochrony, and geometric morphometric analysis of growth models. J Exp Zool B Mol Dev Evol 302:322–340.
Zollikofer CPE, Ponce de León MS. 2010. The evolution of hominin ontogenies. Semin Cell Dev Biol 21:441–452.